IN-05
61939
p. 17

NASA Technical Memorandum 104120

FLUTTER SUPPRESSION VIA PIEZOELECTRIC ACTUATION

Jennifer Heeg

September 1991

National Aeronautics and Space Administration

Langley Research Center
Hampton, Virginia 23665-5225

ABSTRACT

Experimental flutter results obtained from wind-tunnel tests of a two degree of freedom wind-tunnel model are presented for the open- and closed-loop systems. The wind-tunnel model is a two-degree-of-freedom system which is actuated by piezoelectric plates configured as bimorphs. The model design was based on finite element structural analyses and flutter analyses. A control law was designed based on a discrete system model; gain feedback of strain measurements was utilized in the control task. The results show a 21-percent increase in the flutter speed.

INTRODUCTION

During the past 20 years, there has been considerable research to develop active flutter suppression concepts which use conventional leading and trailing edge aerodynamic control surfaces. Because of the catastrophic nature of flutter, a failure of the system could affect flight safety. Therefore, system redundancy, reliability, and maintainability are important issues to be addressed before active flutter suppression can become a common practice in today's aerospace industry or military. To a lesser extent, the control surface authority available to maneuver the aircraft with the simultaneous implementation of active flutter suppression also needs further investigation. To alleviate this concern, alternative active flutter suppression concepts are being studied. The use of embedded actuators made out of adaptive materials for use as secondary controllers has been the focus of many recent research efforts and just recently for flutter suppression purposes. The research presented here focuses on the subcategory of piezoelectric materials.

A material which, when subjected to a mechanical load, produces an electric charge is said to have piezoelectric properties. There are polymers, ceramics, and naturally occurring crystals which have been invented or discovered which exhibit piezoelectric characteristics. A piezoelectric material can be produced from certain types of ceramics and polymers by applying a large electrical field across the material. This induces an orientation of the ions such that the positive and negative poles of the individual ions are aligned with the applied field, denoted the 3-direction. After the poling of the material has taken place, subsequent smaller voltages applied in the same direction as the poling voltage cause the material to expand in this direction. Reversing the polarity of the applied field causes the material to flatten relative to this axis. In the same manner as the Poisson effect, expansion occurs in the in-plane dimensions when the element is flattened in the 3-direction, and likewise, an inplane contraction occurs when the element is thickened. These characteristics allow for the creation of bending elements in which one piezoelectric plate is positioned on the top surface and one on the bottom surface of a thin specimen. One plate is used in contraction while the other is used in extension. The net result is a bending displacement much greater than the length deformation of either of the two layers.[1] This secondary Poisson-like effect will be the primary means of mechanization in the investigation described herein.

Coupling between mechanical stresses and electrical fields is analytically represented by constitutive relationships which contain both the electrical quantities and the mechanical quantities. These equations are often likened to the constitutive relationships applicable to mechanical systems under temperature loads. For example, a temperature distribution applied to a structure generates thermal strains. The same behavioral model can be used to discuss piezoelectricity, where the electrical field applied is analogous to the change in temperature. The thermal expansion coefficients are replaced by the electromechanical coupling coefficients.[2,3]

Polymers, while very useful in generating the piezoelectric effect required for sensor applications, are relatively ineffective in producing the converse piezoelectric effect required for an actuating mechanism.[4] Using crystals has been discarded due to a lack of uniformity and also the full population of the electromechanical coupling matrix. The material properties of Lead Zirconate Titinate (PZT), the piezoelectric ceramic used in this study, are detailed in reference 5. Therefore, ceramics have been chosen for use in this investigation.

OBJECTIVE

While there has been some analytical work performed to determine the feasibility of applying piezoelectric ceramics to suppress flutter, reference 2, there has not been an experiment to date which demonstrates this capability. The fundamental objective of the research presented here is to experimentally suppress flutter using piezoelectric actuators. This report provides a brief overview of the project and presents details concerning finite element and aeroelastic modeling, flutter analyses and control law design, experimental equipment, and test results.

ANALYTICAL MODEL

Finite Element Modeling

A NASTRAN[6] finite element model of the wind-tunnel model and the two-degree-of-freedom mount system (figure 1) was constructed and analyzed. Plate elements were used to represent the spring tines. The plunge spring boundary conditions were modeled as guided ends, that is, zero slope where the plates connect to solid boundaries. The pitch spring tine plate elements were assumed to have cantilevered beam boundary conditions. Observations of the pitch spring behavior and frequency data indicated that the boundary condition was stiffer than that of an ideal cantilever and not as stiff as a guided end. This led to the addition of a torsional spring with a stiffness of half of the difference between these two ideal models. The locations on the spring tines where piezoelectric plates were bonded were defined as composite layers, where the layers of piezoelectric ceramic utilized temperature-dependent material property capabilities of the code. The parallel constitutive relations of thermal-mechanical and electro-mechanical systems allows the voltage applied to the ceramics to be represented by temperature within the finite element code. The aluminum portion of the wing and the clamping block at the free end of the plunge tines were modeled with solid elements. A balsa wood extension of the wing and mass ballast were incorporated as concentrated mass elements placed at their respective centers of gravity.

A modal analysis was performed to generate natural frequencies and mode shapes. The vibration mode shapes are shown in figure 2; the first mode, designated plunge due to the dominance of translational motion, was predicted to occur at a natural frequency at 7.8 Hz. The second mode, which is characterized by the pitching of the airfoil relative to the mount system, was predicted at a natural frequency of 10.9 Hz.

Studies were also performed using the finite element model to define the placement of the piezoelectric actuating plates for maximum effect and to determine the amount of mass ballast needed to create a low speed flutter condition.

Aeroelastic Modeling

Classical open-loop aeroelastic equations of motion, based on the coupled plunge and pitch degrees of freedom, were formulated using Lagrange's energy method. These equations represent the summation of inertial, dissipative, and internal restorative forces along with the reduced-

frequency dependent aerodynamic forces which are induced by the structural motion and control forces. The piezoelectric force was also incorporated into the governing equations of motion.

The unsteady aerodynamics were calculated at Mach .05 using the Doublet Lattice Aerodynamic Theory[7] as implemented in the Aeroelastic Vehicle Analysis (AVA) system of computer modules. This is a lifting surface theory and requires, as input, the natural modes and a set of aerodynamic panels and boxes to represent the geometry. The box pattern consisted of 5 chordwise and 10 spanwise strips of boxes for a total of 50 boxes. AVA provides generalized aerodynamic forces (GAFs) in the form of reduced frequency dependent matrices. For control law design, and to make use of modern state-space techniques, the GAFs were approximated using rational functions of the Laplace variable. The aeroelastic equations could then easily be transformed into first-order state-space equations of motion.[8]

The mode shapes used in the analysis were normalized such that the generalized mass matrix associated with the structure was the identity matrix. The structural damping values used in the analyses were determined experimentally to be .034 for the plunge mode and .11 for the pitch mode.

Flutter Analysis

Matched point flutter analyses were performed at sea level. The velocity root locus shown in figure 3 illustrates the open-loop flutter characteristics of the model.[9] The predicted flutter mechanism is a coalescence of the two modes of the system at a velocity of 560 inches per second at 9.1 Hz.

CONTROL LAW

Illustrated in figure 4 for a gain feedback control law, the control computer introduces its own dynamics into the feedback path. The digital controller implementation scheme shifts the output data by one sample and applies a zero-order hold. As the sample rate is varied, the frequency response of the digital controller changes. By using a sample rate which emulates the phase characteristics of analog derivative feedback near the frequency of control interest allows the system to simulate derivative feedback, despite having only displacement measurements. The current control law utilizes the dynamics of the implementation scheme, requiring only gain feedback. The frequencies of concern lie between 7.9 and 11.1 Hz. An examination of figure 5 shows that for a 20 Hz sample rate, the dynamics of the controller induce an approximate derivative behavior in this frequency range.[10]

Strain is measured on the model by a bridge powered at 5 volts, amplified by 100 and input to the digital computer at 20 samples per second. A gain of -33 is the only compensation explicitly programmed. The output is delayed by one sample and then amplified by 25 before being sent to the piezoelectric plates. Including the strain gage factor of 2.075, the system gain between the voltage to the piezoelectric actuator and strain gage on the spring tine is about -9×10^{5}.

EXPERIMENTAL APPARATUS

Wind Tunnel

The Flutter Research and Experiment Device (FRED) shown in figure 6, is an open circuit table-top wind tunnel with a maximum operating velocity of 85 miles per hour, approximately 1500 inches per second. The test section is 6 inches by 6 inches and is constructed of plexiglass

for model viewing. The flow is pulled through the tunnel by a 2 horsepower motor and smoothed by a single honeycomb screen at the beginning of the contraction duct. Models are mounted from the removable ceiling of the test section.

Mount System

The mount system, shown in figure 7, has two degrees of freedom - plunge and pitch. The apparatus is exterior to the wind tunnel and suspends the wing by two pins through slots in the test section ceiling.

The plunge mechanism consists of two spring steel plates or tines separated by .75 inches and clamped at both ends to maintain this distance. This provides the pure plunging motion of a beam with guided boundary conditions instead of the flapping motion associated with a cantilevered beam. The pitch mechanism is a single spring tine connected to the wing at the leading edge and at the .24 chord location, where there is a bearing-like mechanism which allows for free rotation. This configuration provides the wing with pitch stiffness and a pitch axis. The two mechanisms are joined together as shown in figure 8. The forward end of the pitch mechanism is fixed relative to the plunge springs by mounting the pitch pivot pin to the lower clamping block of the plunge mechanism.

The mount system was designed such that each degree of freedom could be controlled as independently as possible from the other mode. Additionally, each degree of freedom is controlled by leaf springs, which provide flat surfaces to which sheets of piezoelectric ceramics can be affixed.

Wing

The wing, depicted in figure 9, consists of three sections: an aluminum primary structure, a balsa wood extension, and an aluminum mass ballast. The primary wing structure is formed from a one-eighth inch thick isotropic aluminum plate with a diamond cross-section, blunted leading and trailing edges and a flat midchord section. It has a chord of 2 inches, with the pitch pivot at the midchord. The balsa wood extension overlays the aft half of the primary structure and extends the chord length to 4.25 inches. The trailing edge of this section was coated with aluminum to provide a mass ballast. The mass of the entire wing is .090 lbm and has an inertia about the pitch axis of 1×10^{-6} lbm-square inches. All three sections extend the full span of the wing, which is 4 inches.

Piezoelectric Actuators

Four sets of piezoelectric ceramic plates were installed to actuate the test article. Two plates are bonded to opposing sides of the plunge spring tine, (figure 10), with their poles both oriented towards the steel, to form an actuator. The plates are electrically isolated from the steel by the bonding layers. Small copper tabs, affixed beneath the plates during the bonding process, serve as the means of applying voltages to the bonded-side electrodes. Only one set of actuating plates, located near the root of one plunge tine was used as a feedback controller.

Digital Controller/Data Acquisition System

The control laws are implemented using a personal computer, with a 80386 processor and 80387 co-processor running a real-time Unix operating system.[11] The control laws are programmed in the C language and use floating point arithmetic for all control law calculations. The data acquisition system uses 12-bit analog-to-digital converters with a sample rate up to 500 Hz for a gain feedback single input/single output control law.

Experimental Test Setup

The wind tunnel and model had three sensor systems: a strain gage bridge, a linear accelerometer, and a hot wire anemometer. The first two were used as input to the digital controller. The strain gage bridge was mounted at the base of a plunge spring tine. The accelerometer served as a roving measurement, being placed where applicable for different experiments. During zero airspeed testing, it was located on the airfoil, however, during flutter testing it was installed on the clamping block. Both the strain and the acceleration were amplified by 100 before being sent to the analog-to-digital converters. The output voltage of the controller was sent to an operational amplifier having a gain of 25 and a limit on the output voltage of 80 volts. This limited the usable range of output values from the controller to +/- 3.2 volts. The amplified voltage was then applied across each of the piezoelectric elements.

EXPERIMENTS

System Identification

There were several techniques, both experimental and analytical, used to extract system parameters. Impulse response functions of the accelerometer, generated by hammer tests, proved to be the most reliable means of extracting the natural frequencies of the system, but could be used only at zero airspeed due to the lack of access to the model while in the tunnel and the amount of disturbance introduced to the flow by the presence of the accelerometer and its lead wire. The power spectral density plot generated by this technique, shown in figure 11, indicates that the natural frequencies are 7.9 and 11.1 Hz. The structural damping of the plunge mode was also determined from this data by taking the ratio of the frequency width of the peak at the half amplitude and the natural frequency. The damping ratio is half of this value, .017. The damping of the pitch mode at zero airspeed was determined by plucking the airfoil, displacing it primarily in pitch. The ensuing response, shown in figure 12, was analyzed using the logarithmic decrement technique to obtain a value of .055 damping ratio.

Open Loop Flutter Testing

The risks associated with flutter testing are minimized in this experiment due to the unique design of the test article. Because the mount system is located exterior to the tunnel and the model is small, it is possible to stop flutter by manually taking hold of the flexible springs or the clamping block.

The flutter tests were conducted by increasing the velocity and allowing the model to sit at the tunnel condition for several minutes. The turbulence within the tunnel was relied upon to be sufficient to perturb the model. Flutter was encountered at 580 inches per second; the frequency of the oscillation was 9.6 Hz.

Closed Loop Flutter Testing

The loop was closed while the wind tunnel was below the flutter velocity. Proceeding in the same manner as the open-loop flutter testing, the speed was increased until flutter occurred. Two additional tests of interest were performed. The first test demonstrated that once unaugmented flutter was encountered, turning on the controller was not sufficient to damp the motion. The second test illustrated that when the control law was turned off above the open-loop flutter velocity, divergent oscillations immediately began. The use of the feedback system resulted in a flutter speed increase of 21 percent (figure 13).

CONCLUSIONS AND FUTURE WORK

The use of piezoelectric actuators has been demonstrated as a mechanism to suppress flutter. A mount system has been designed such that plate-type actuators can be utilized. The future work will focus on assessing the tools and equations used to predict the actuator effectiveness and also on an expanded experimental program which will include a flexible aerodynamic structure and a tradeoff study with conventional control surfaces.

REFERENCES

1. Anderson, E. H.; and Crawley, E. F.: Piezoceramic Actuation of One- and Two- Dimensional Structures, Space Systems Laboratory, Massachusetts Institute of Technology, Cambridge, MA, 1989.

2. Scott, R. C.: Control of Flutter using Adaptive Materials, Master's Thesis, Purdue University, May 1990.

3. Barrett, R.: Intelligent Rotor Blade and Structures Development Using Directionally Attached Piezoelectric Crystals, M.S. Thesis University of Maryland Department of Aerospace Engineering, 1990.

4. Spangler, R. L.: Piezoelectric Actuators for Helicopter Rotor Control, Master's Thesis, Massachusetts Institute of Technology, February 1989.

5. Product Information Catalog, PiezoSystems Solid State Motion Technologies, May 1990.

6. MSC/NASTRAN User's Manual Version 65, The MacNeal Schwendler Corporation, November 1985.

7. Rodden, W. P.; Giesing, J. P.; and Kalman, T. P.: New Developments and Applications of the Subsonic Doublet-Lattice Method for Nonplanar Configurations, AGARD Symposium on Unsteady Aerodynamics for Aeroelastic Analyses of Interfering Surfaces, Paper Number 4, November 1970.

8. Mukhopadhyay, V.; Newsom, J. R.; and Abel, I.: A Method for Obtaining Reduced-Order Control Laws for High-Order Systems Using Optimization Techniques, NASA Technical Paper 1876, 1981.

9. Tiffany, S. H.; and Adams, W. M., Jr.: Nonlinear Programming Extensions to Rational Function Approximation Methods for Unsteady Aerodynamic Forces, NASA Technical Paper 2776, July 1988.

10. Kuo, B. C.: Digital Control Systems, Holt, Rinehart and Winston, Inc., 1980.

11. Dunn, H. J.: Experimental Results of Active Control on a Large Structure to Suppress Vibration, Proceedings AIAA Guidance, Navigation, and Control Conference, New Orleans, Louisiana, 1991.

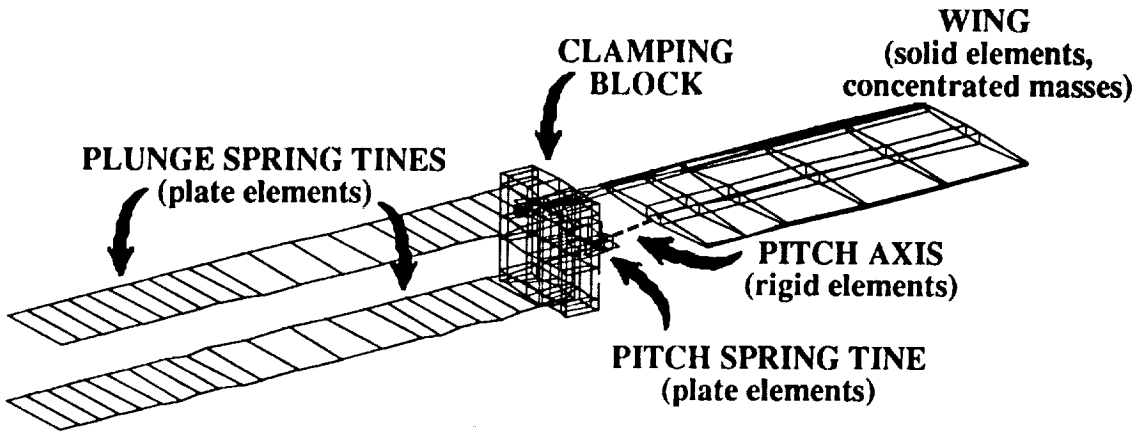

Figure 1.- Finite element model.

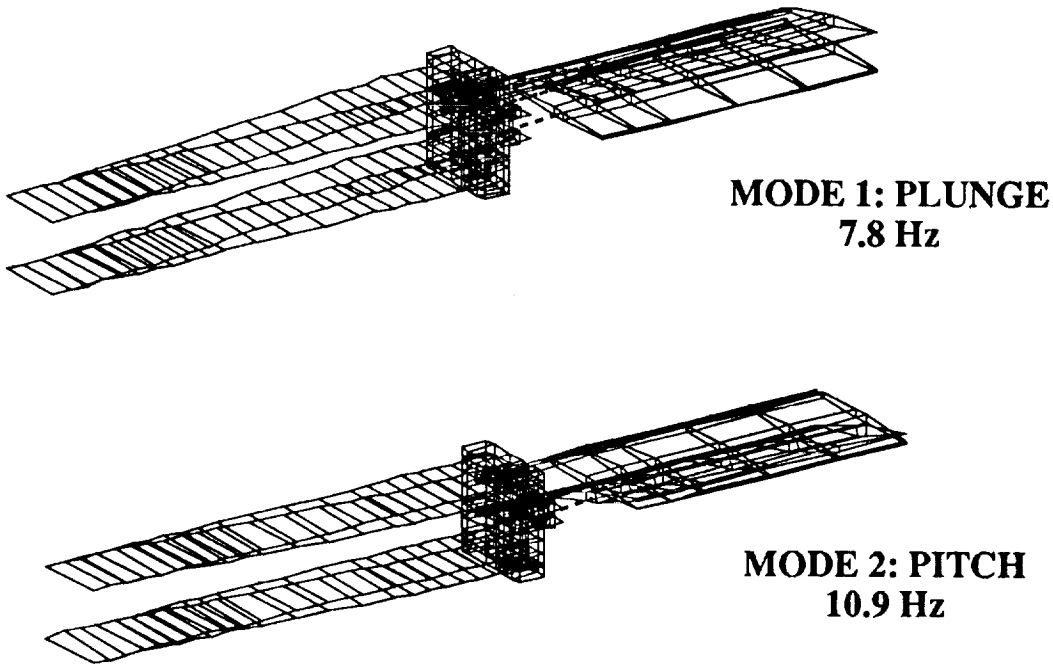

Figure 2.- Finite element analysis vibration mode shapes.

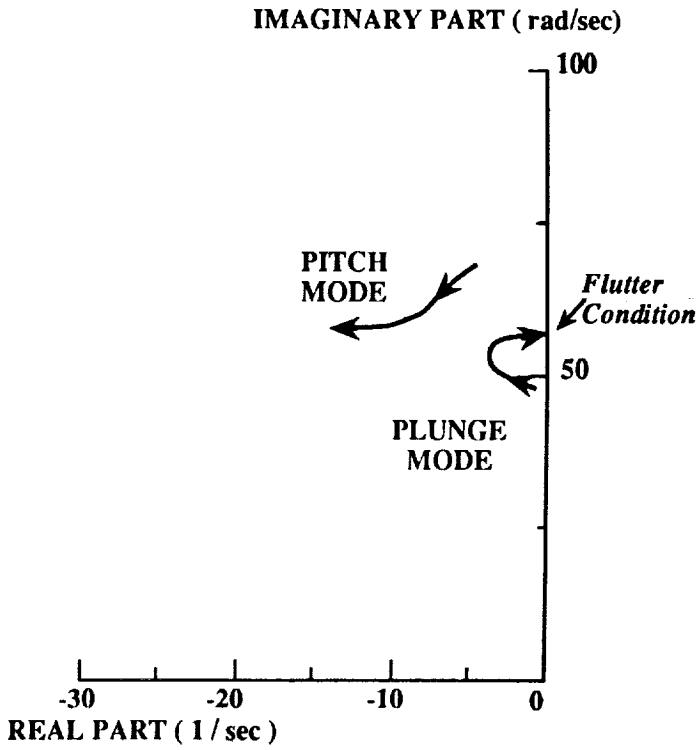

Figure 3.- Root locus - Eigenvalue locations as velocity is varied.

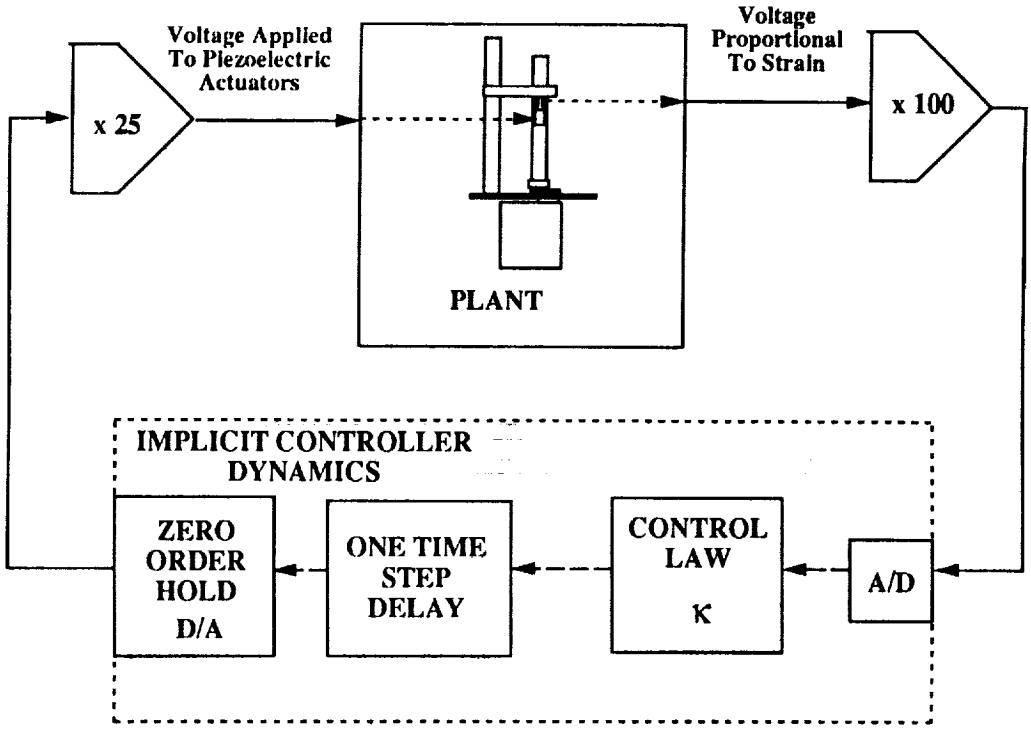

Figure 4.- Block diagram of closed-loop system.

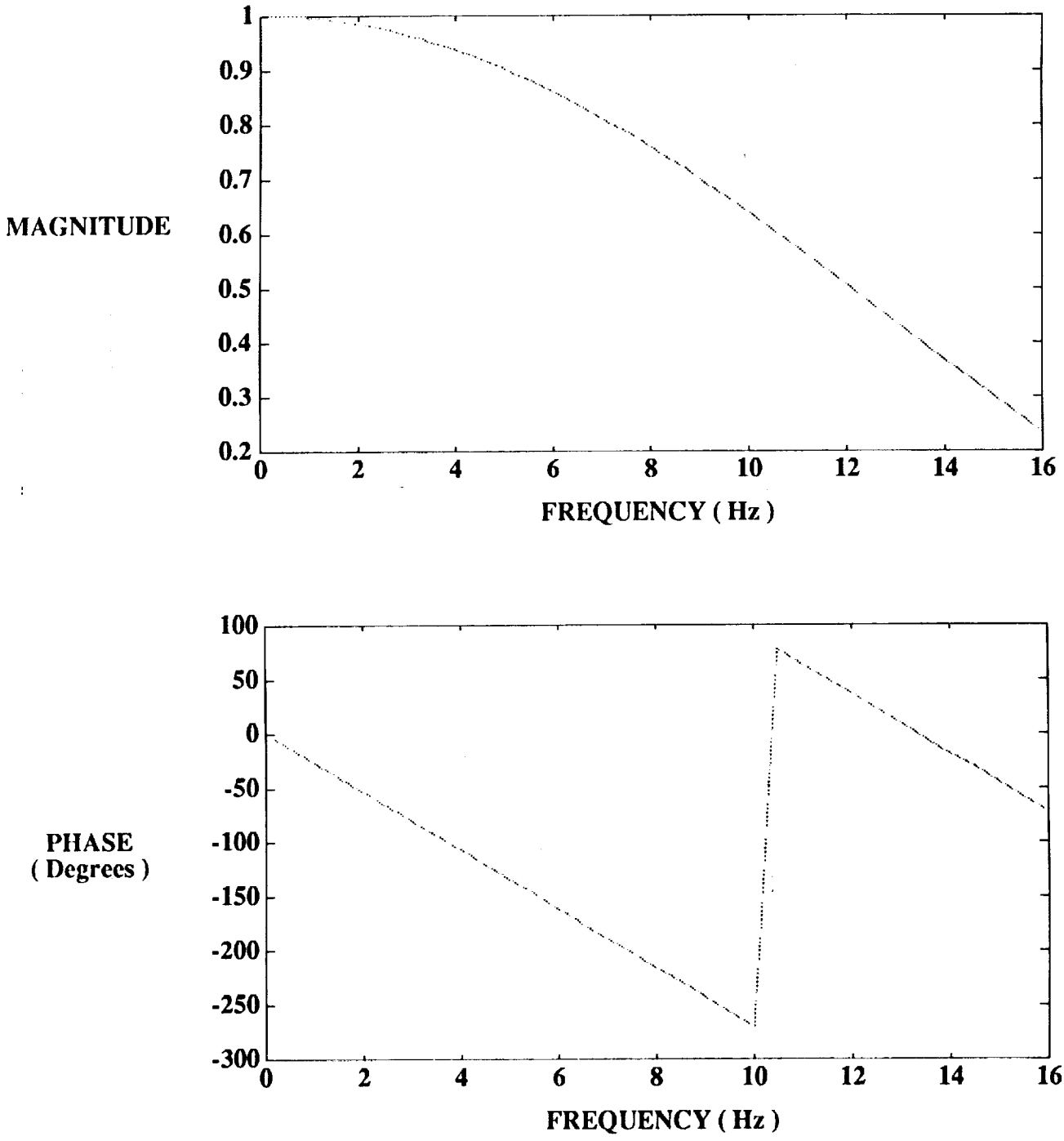

Figure 5.- Frequency response plot of implicit controller dynamics for 20 Hz sample rate (time delay and zero order hold).

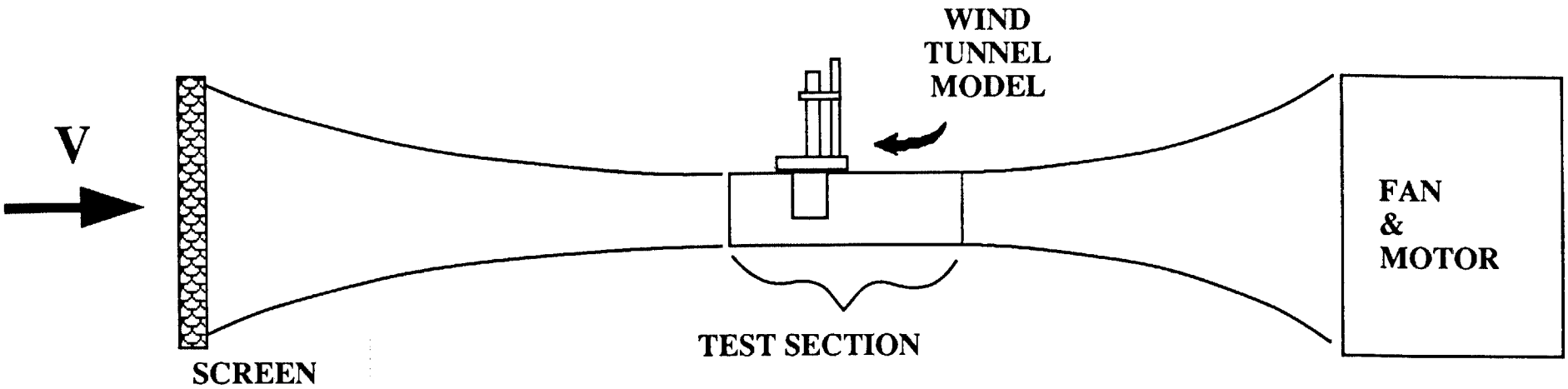

TEST SECTION: 6 INCHES BY 6 INCHES

CEILING MOUNTING FOR MODELS

LIMITS: VELOCITY -- 1500 in/s (85 mph)

DYNAMIC PRESSURE -- 0.13 psi

Figure 6.- Schematic of Flutter Research and Experiment Device (FRED) wind tunnel.

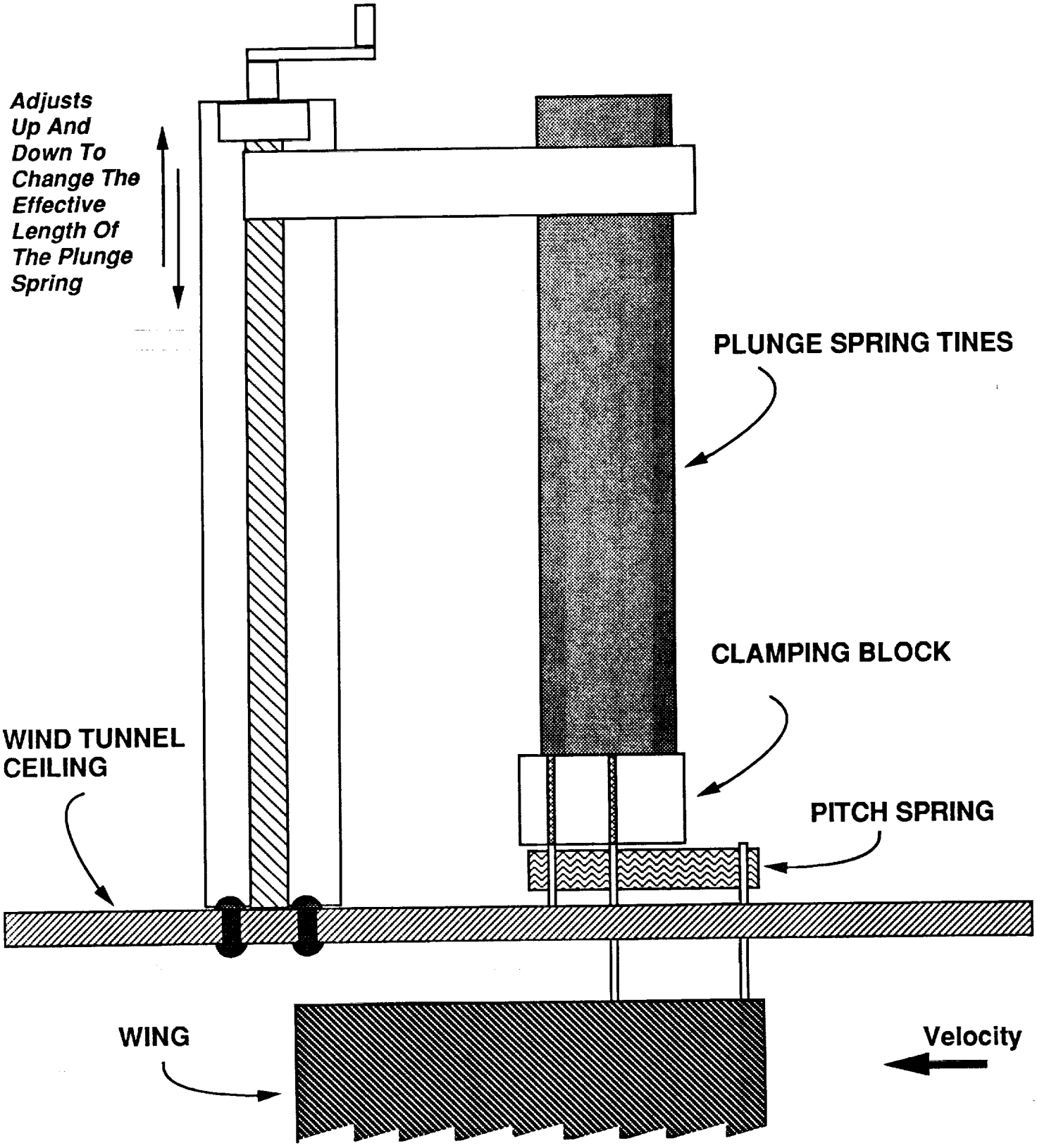

Figure 7.- Wind-tunnel mount system (not to scale).

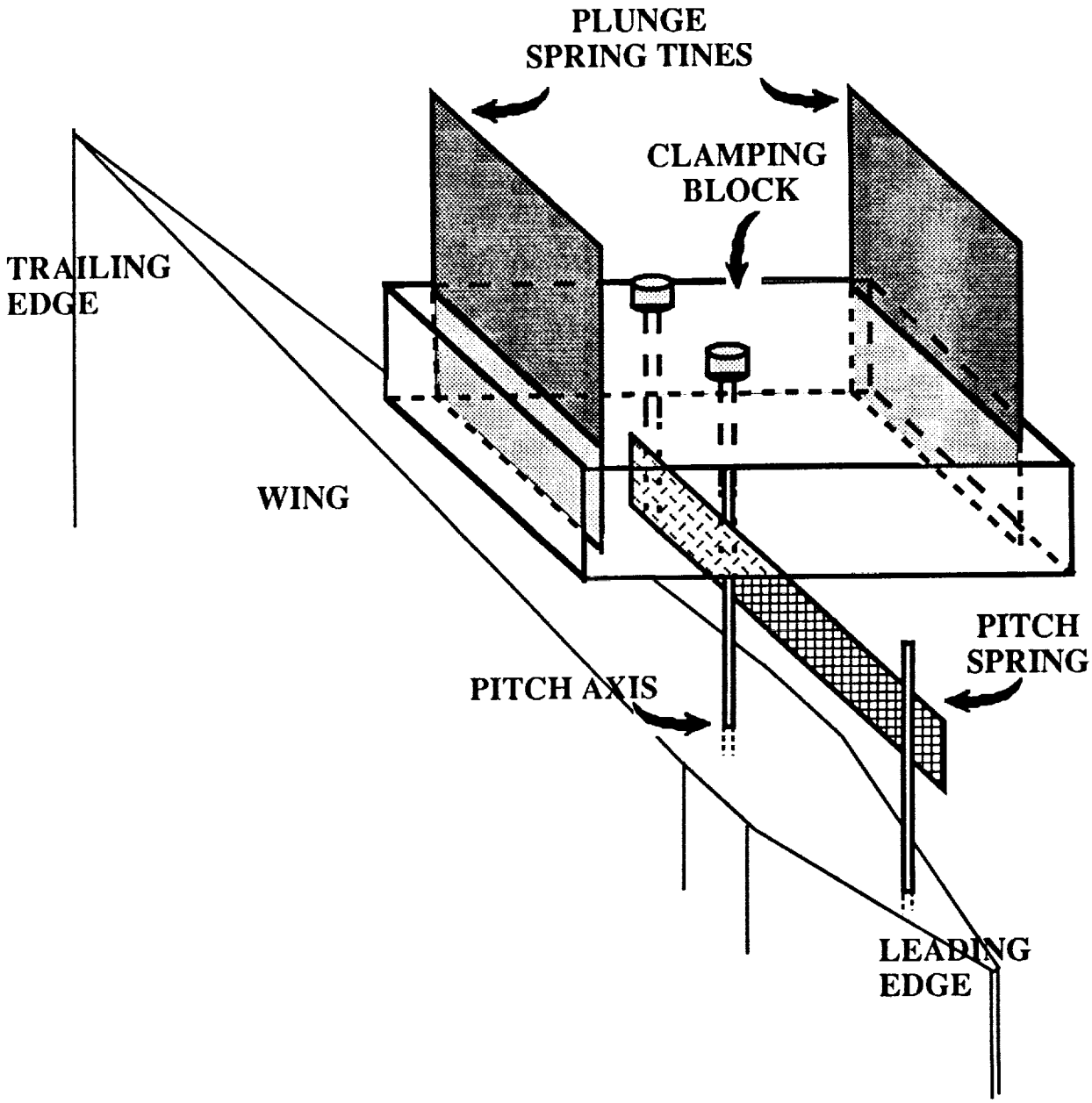

Figure 8.- Mount system closeup interconnection mechanism for the plunge and pitch degrees of freedom.

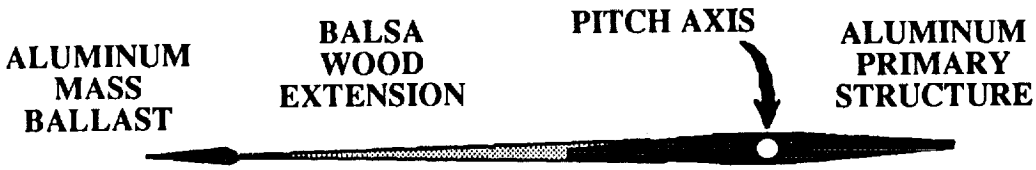

Figure 9.- Wing, cross-sectional view.

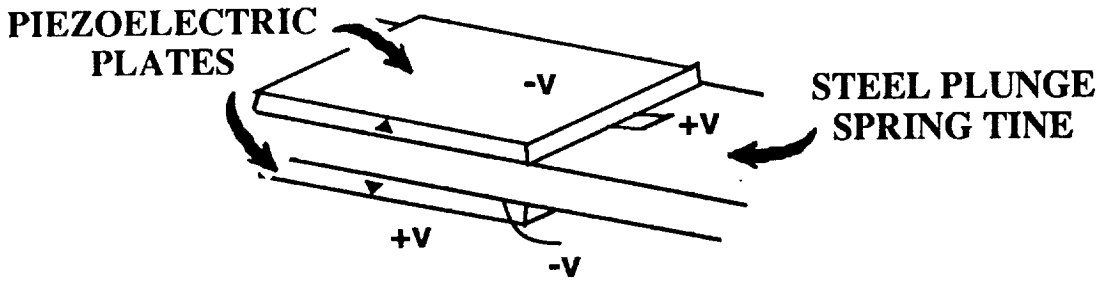

Figure 10.- Piezoelectric actuator attachment to plunge spring tine.

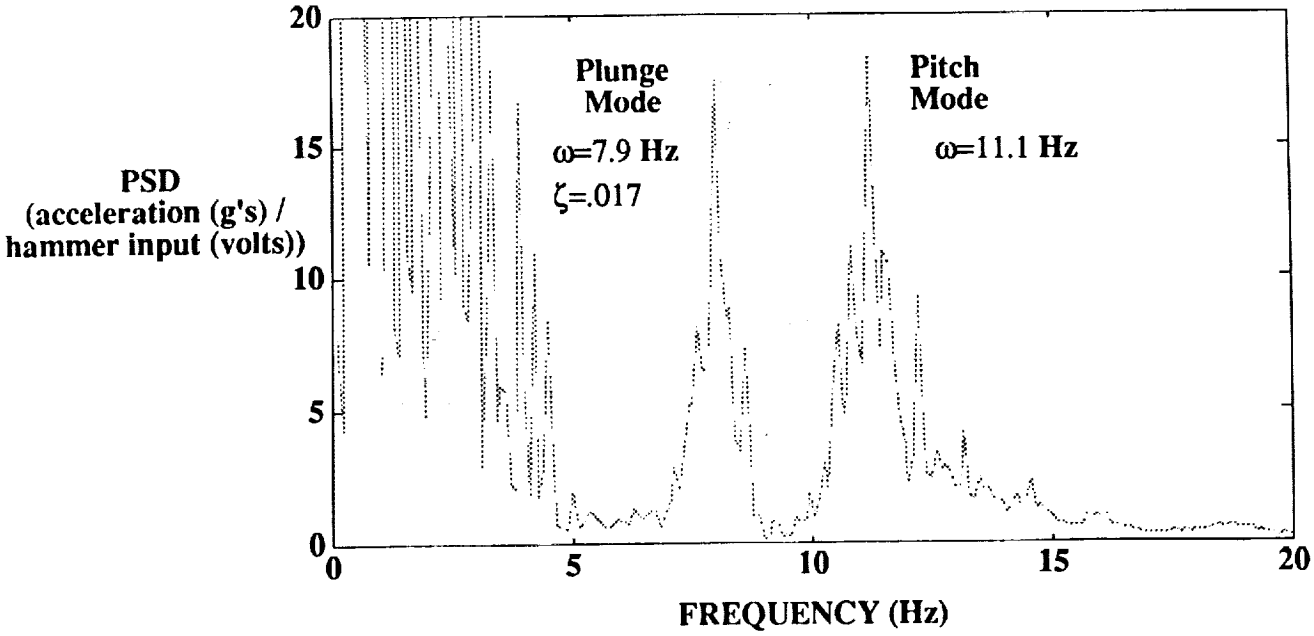

Figure 11.- Power spectral density of acceleration response to hammer taps at zero airspeed.

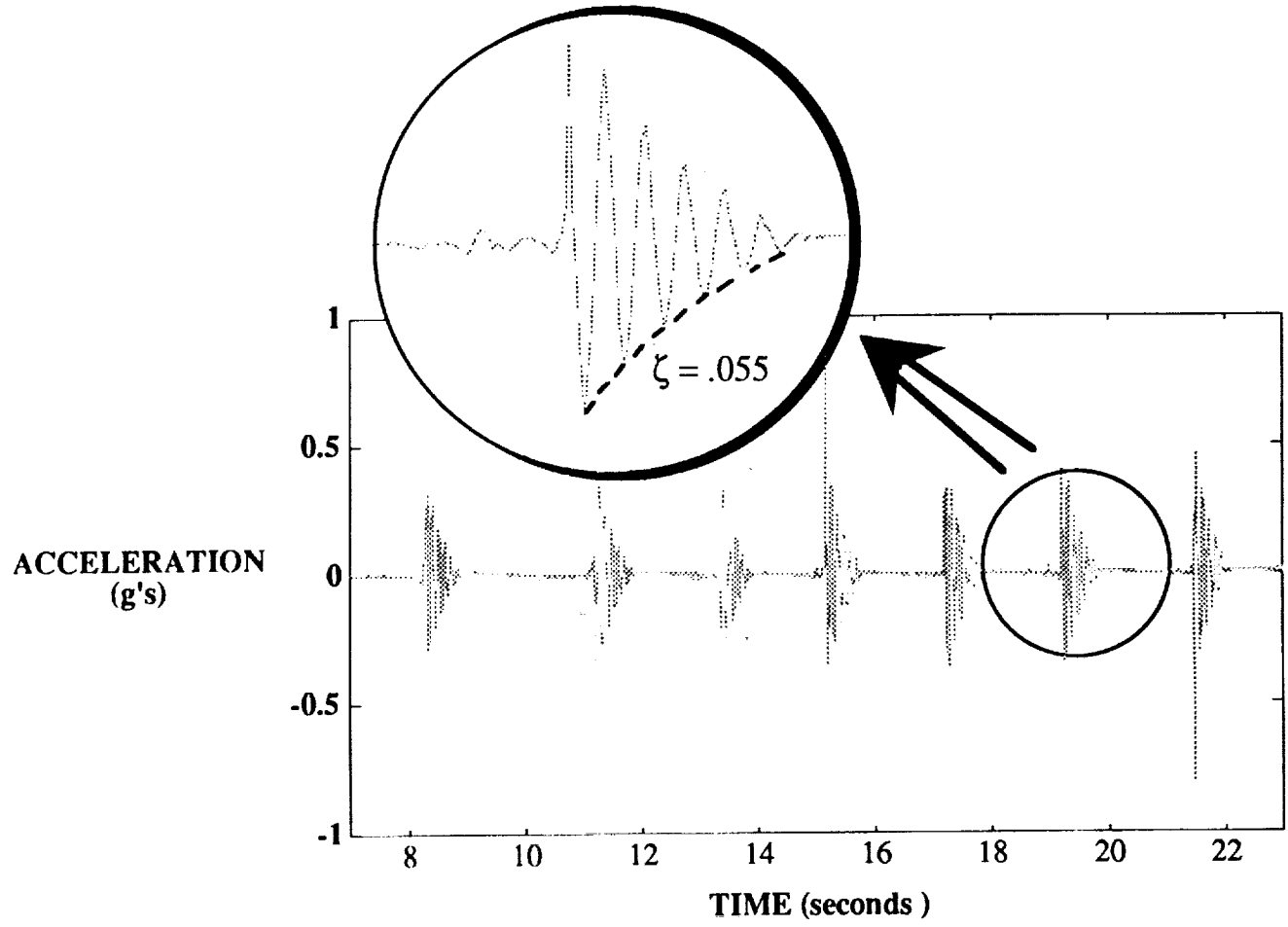

Figure 12.- Time history of acceleration response to plucks at zero airspeed.

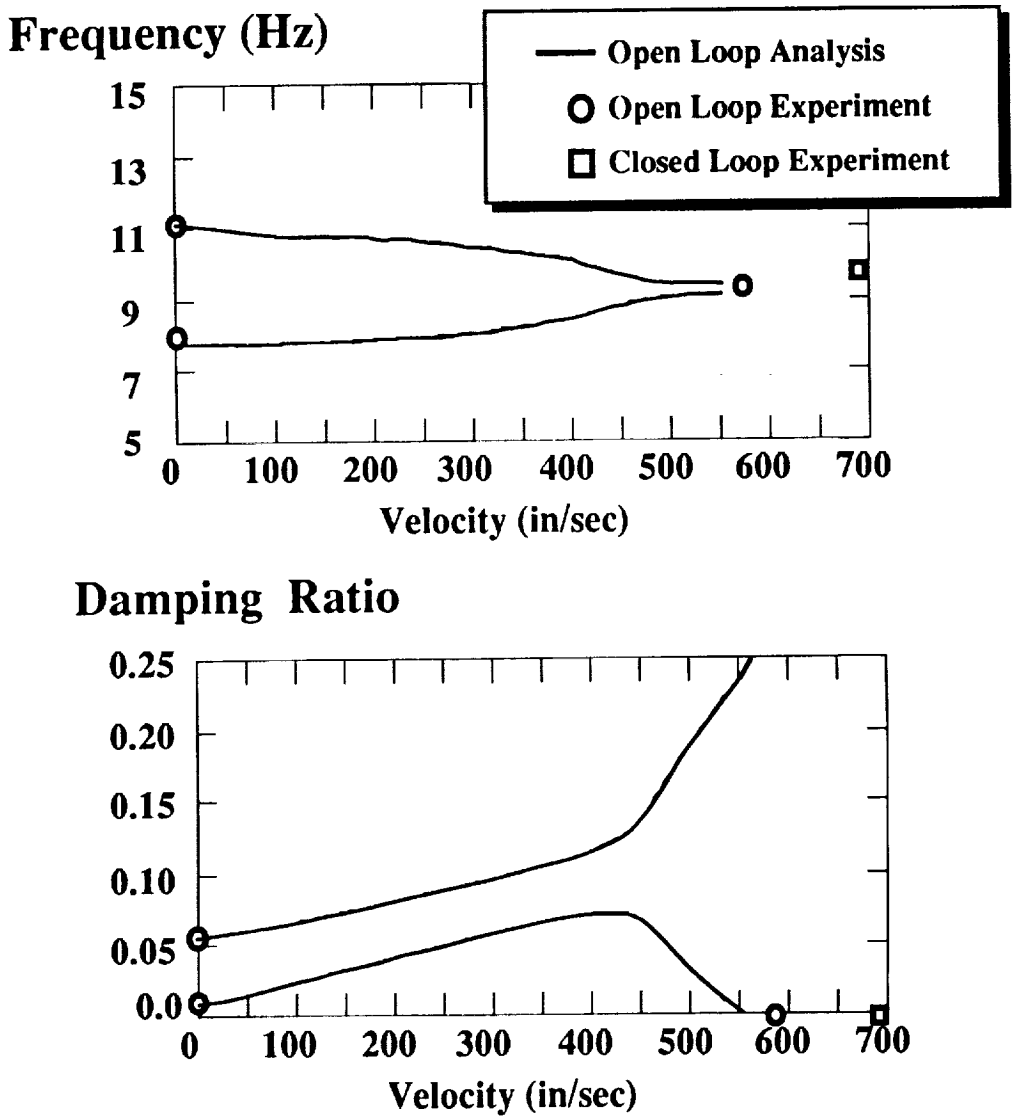

Figure 13.- Analytical and experimental flutter results.

NASA National Aeronautics and Space Administration

Report Documentation Page

1. Report No.	2. Government Accession No.	3. Recipient's Catalog No.
NASA TM-104120		

4. Title and Subtitle	5. Report Date
Flutter Suppression Via Piezoelectric Actuation	September 1991
	6. Performing Organization Code

7. Author(s)	8. Performing Organization Report No.
Jennifer Heeg	10. Work Unit No. 505-63-50-15

9. Performing Organization Name and Address	11. Contract or Grant No.
NASA Langley Research Center Hampton, VA 23665-5225	13. Type of Report and Period Covered

12. Sponsoring Agency Name and Address	14. Sponsoring Agency Code
National Aeronautics and Space Administration Washington, DC 20546-0001	Technical Memorandum

15. Supplementary Notes

16. Abstract

Experimental flutter results obtained from wind-tunnel tests of a two degree of freedom wind-tunnel model are presented for the open- and closed-loop systems. The wind-tunnel model is a two-degree-of-freedom system which is actuated by piezoelectric plates configured as bimorphs. The model design was based on finite element structural analyses and flutter analyses. A control law was designed based on a discrete system model; gain feedback of strain measurements was utilized in the control task. The results show a 21-percent increase in the flutter speed.

17. Key Words (Suggested by Author(s))

Adaptive Structures
Aeroservoelasticity
Flutter Suppression
Piezoelectric

18. Distribution Statement

Unclassified - Unlimited

Subject Category - 05

19. Security Classif. (of this report)	20. Security Classif. (of this page)	21. No. of pages	22. Price
Unclassified	Unclassified	16	A03